Interferon-γ facilitates hepatic antiviral T cell retention for the maintenance of liver-induced systemic tolerance

Zhutian Zeng,[1]* Lu Li,[1,2]* Yongyan Chen,[1] Haiming Wei,[1] Rui Sun,[1] and Zhigang Tian[1,2,3]

[1]Institute of Immunology and the Key Laboratory of Innate Immunity and Chronic Disease, Chinese Academy of Science, School of Life Sciences and Medical Center, University of Science and Technology of China, Hefei 230027, China
[2]Hefei National Laboratory for Physical Sciences at the Microscale, Hefei 230027, China
[3]Collaborative Innovation Center for Diagnosis and Treatment of Infectious Diseases, State Key Laboratory for Diagnosis and Treatment of Infectious Diseases, First Affiliated Hospital, College of Medicine, Zhejiang University, Hangzhou 310003, China

Persistent exposure to liver pathogens leads to systemic antigen-specific tolerance, a major cause of chronicity during hepatotropic infection. The mechanism regarding how this systemic tolerance is maintained remains poorly elucidated. In a well established mouse model of hepatitis B virus (HBV) persistence–induced systemic tolerance, we observed that interferon-γ (IFN-γ) deficiency led to complete loss of tolerance, resulting in robust anti-HBV responses upon peripheral vaccination. The recovery of vaccine-induced anti-HBV responses was mainly caused by the retained antigen-specific CD4+ T cells rather than decreased functional inhibitory cells in the periphery. Mechanistically, HBV persistence induced sustained hepatic CD4+ T cell–derived IFN-γ production. IFN-γ was found to promote CXCL9 secretion from liver-resident macrophages. This T cell chemokine facilitated the retention of antiviral CD4+ T cells in the liver in a CXCR3-dependent manner. Hepatic sequestrated antiviral CD4+ T cells subsequently underwent local apoptotic elimination partially via cytotoxic T lymphocyte–associated protein 4 ligation. These findings reveal an unexpected tolerogenic role for IFN-γ during viral persistence in the liver, providing new mechanistic insights regarding the maintenance of systemic antigen-specific tolerance during HBV persistence.

The most mysterious feature of the liver as an immune organ is that it favors the induction of tolerance rather than immunity during exposure to foreign antigens (Crispe, 2009). In this regard, the following two features of liver immune tolerance are known: first, the liver works as an immune-privileged site, tending to accept allografts (Calne et al., 1969), hepatotropic pathogens (Protzer et al., 2012), and liver-targeted exogenous proteins (LoDuca et al., 2009); second, the liver may induce systemic tolerance characterized by systemic unresponsiveness toward antigens that are persistently expressed in the liver. This latter feature has been shown to possess tremendous clinical potential; for example, liver allografts preferentially reduce immune rejection against subsequent skin transplants from the same donor (Calne et al., 1969), and hepatic expression of an autoantigen significantly reduces the incidence of autoimmune disease (Lüth et al., 2008). Thus, exploring the mechanisms of liver-induced systemic tolerance will undoubtedly provide useful insights that can be of great help in developing strategies to treat human diseases.

Hepatic antigen-presenting cells (e.g., Kupffer cells and liver sinusoidal endothelial cells) are well characterized tolerance-inducing cells because of both their insufficient delivery of costimulatory signals and their tendency to produce immune inhibitory molecules, leading to an inherent intrahepatic tolerogenic microenvironment in the steady state (Thomson and Knolle, 2010). The outcome of an immune response inside the liver is delicately determined by the extent of inflammation. In conditions of chronic inflammation or low-grade inflammation when the immunosuppressive microenvironment is dominant, the liver may act either as a "graveyard" for effector cells (Crispe et al., 2000) or as a "school" to educate regulatory cells (Li and Tian, 2013). These processes can lead to clonal deletion (Dobrzynski et al., 2004; Dong et al., 2004) or inhibition of peripheral antigen-specific T cells (Cao et al., 2007; Breous et al., 2009; Xu et al., 2013), which are the principal mechanisms underlying liver-induced antigen-specific tolerance. However, the manner in which these mechanisms are orchestrated to maintain extrahepatic systemic tolerance during viral persistence in the liver is largely unknown. Moreover, the precise mediators controlling the induction or maintenance of liver-induced systemic tolerance have rarely been reported, but their identification is critical for developing therapeutic intervention strategies. IFN-γ is primarily known as an important effector molecule for antiviral T cells, but it can also exert immune-regulatory functions such as the induction of activation-induced T cell death (Refaeli et al., 2002), antitumor T cell apoptosis (Berner et al., 2007), and the generation of regulatory T cells (Wang et al., 2006). Thus,

---

*Z. Zeng and L. Li contributed equally to this paper.
Correspondence to Zhigang Tian: tzg@ustc.edu.cn

Abbreviations used: CBA, cytometric bead array; CHB, chronic HBV; GC, germinal center; HBcAg, HBV core antigen; HBeAg, HBV e antigen; HBsAg, HBV surface antigen; HBV, hepatitis B virus; LNPC, liver nonparenchymal cell.

The Journal of Experimental Medicine

these IFN-γ–mediated effects on T cells may align with the T cell dysfunction observed in liver tolerance, hinting at the possibility that IFN-γ may play a role in liver tolerance.

Chronic hepatitis B virus (HBV [CHB]) carriers are at a high risk of disease progression (Protzer et al., 2012). During HBV persistence, peripheral HBV-specific responses are greatly diminished because of liver-induced systemic tolerance (Rehermann and Nascimbeni, 2005). Consequently, CHB carriers are hyporesponsive to HBV vaccination, making it extremely difficult to design an effective therapeutic vaccine against HBV (Dikici et al., 2003). For that reason, a mouse model mimicking viral persistence in asymptomatic CHB carriers was established (Huang et al., 2006; Lin et al., 2010). In this model, a single injection of HBV-encoding plasmid allows persistent HBV replication and intrahepatic expression of HBV-related antigens in immune-competent adult mice. Most importantly, they cannot respond to peripheral HBV surface antigen (HBsAg) vaccination, thus demonstrating a systemic antigen-specific immune tolerant state similar to CHB carriers and providing a reliable mouse model to study the mechanisms underlying HBV persistence–induced systemic tolerance (Huang et al., 2006; Xu et al., 2013, 2014; Zeng et al., 2013). Using this model, we found that systemic tolerance during HBV persistence is completely abrogated in the context of IFN-γ deficiency. Mechanistically, HBV persistence correlated with sustained IFN-γ production by hepatic CD4+ T cells, which then acted on liver-resident macrophages to promote local CXCL9 secretion. This T cell chemokine subsequently attracted and trapped systemic antiviral CD4+ T cells in the liver to maintain systemic tolerance.

RESULTS

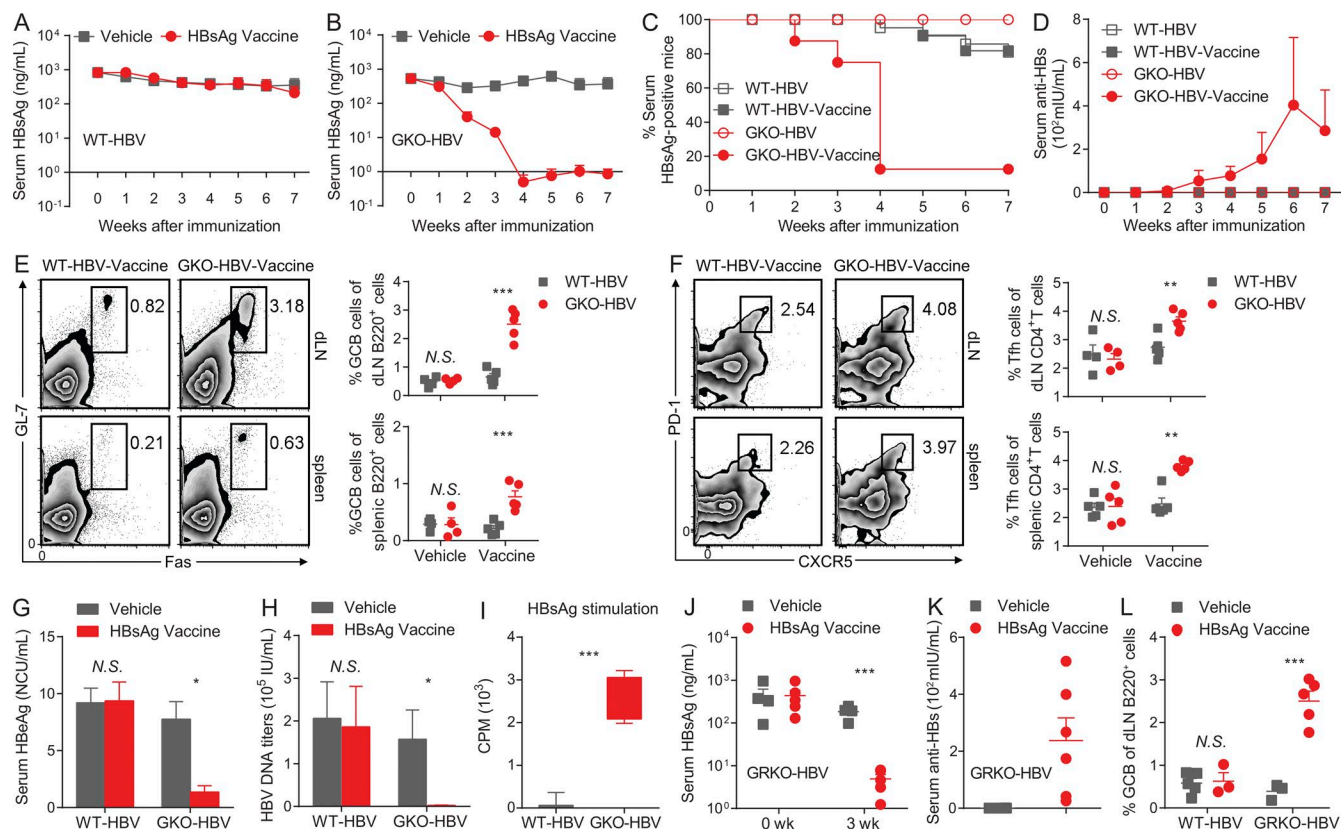### IFN-γ maintains systemic tolerance during HBV persistence

To elucidate the precise role of IFN-γ in liver tolerance, a previously reported hydrodynamic injection–based, HBV-persistent mouse model was used, in which mice persistently express HBV antigens without any liver pathology, rendering them completely tolerant to peripheral HBsAg vaccination (Fig. 1, A, C, and D; Huang et al., 2006; Xu et al., 2013, 2014). IFN-γ–deficient (GKO) mice showed impaired spontaneous clearance of HBV as expected (Fig. 1 C). However, in contrast to WT mice, GKO mice responded robustly toward HBsAg vaccination: they exhibited dramatically reduced serum HBsAg (Fig. 1 B), detectable HBsAg antibody (anti–HBs) titers (Fig. 1 D), and a higher frequency of vaccine-induced germinal center (GC) B cells and follicular helper T cells compared with their WT counterparts (Fig. 1, E and F), thus suggesting that GKO mice lost systemic tolerance toward the HBsAg. Serum HBV e antigen (HBeAg) levels (Fig. 1 G) and HBV DNA titers (Fig. 1 H) also decreased, indicating that vaccination with HBsAg elicited specific anti-HBV immunity against multiple HBV antigens in HBV-carrier GKO mice, similar to the effects observed in HBV-vaccinated naive WT mice. In contrast, splenocytes from HBV-carrier GKO mice, but not WT mice, proliferated in response to HBsAg

stimulation in vitro (Fig. 1 I), which further suggested that the systemic tolerance toward the HBsAg was abolished in HBV-persistent GKO mice. HBV-persistent IFN-γ receptor–deficient (GRKO) mice also robustly reacted against peripheral HBsAg vaccination (Fig. 1, J–L), indicating that intact IFN-γ signaling was indispensable for maintaining systemic tolerance during HBV persistence.

IFN-γ deficiency leads to the preservation of functional HBsAg-specific CD4+ T cells in the periphery

We next explored how IFN-γ might promote tolerance toward HBsAg stimulation. Liver-induced antigen-specific systemic tolerance is usually ascribed to the induction of inhibitory cells, through which tolerance can be transferred into a naive host (Cao et al., 2007; Lüth et al., 2008; Breous et al., 2009; Xu et al., 2013). To test this possibility, we adoptively transferred splenocytes from HBV-carrier WT or GKO mice to naive WT or GKO recipient mice, respectively (Fig. 2, A and B). If the production of anti-HBs in response to vaccination in recipient mice was inhibited by the donor cell transfer, then we could conclude that HBsAg-specific inhibitory cells were present within these donor cells or vice versa. Transferred splenocytes from HBV-carrier GKO or WT mice exhibited a similar level of inhibition of anti-HBs production in recipient mice after HBsAg vaccination (Fig. 2, A and B), indicating that similar amounts of HBsAg-specific inhibitory cells were present in both WT and GKO-HBV mice. Consistently, no reductions of the numbers or functions of CD4+Foxp3+ regulatory T cells (T reg cells) were observed in GKO-HBV mice (Fig. 2, C–G). It is worth noting that GKO mice could overcome HBV-induced systemic tolerance even with a higher frequency of T reg cells than WT mice in spleen (Fig. 2, C–F). Collectively, we supposed that the loss of HBsAg-specific systemic tolerance in HBV-carrier GKO mice was not caused by the reduction or functional impairment of peripheral HBsAg-specific inhibitory cells.

The loss of functional antigen-specific T cell clones is another common reason for liver-induced antigen-specific systemic tolerance (Dobrzynski et al., 2004; Dong et al., 2004). Consequently, we took advantage of the reconstitution of adaptive immune–deficient mice with various donor cells to evaluate the presence of antigen-specific immune cells (Goubier et al., 2008) in HBV-carrier GKO or WT mice. In these adaptive immune-reconstituted mice, the HBsAg-specific response to vaccination (i.e., anti-HBs production) only derived from the donor cells and could be used as a readout both for detecting HBsAg-specific clones and for judging the tolerance state of the donor mice. Rag1−/− mice reconstituted with splenocytes from HBV-carrier GKO mice, but not WT mice showed significant anti-HBs production after vaccination at levels similar to reconstitution with splenocytes from control WT mice that were not preinjected with HBV plasmid (Fig. 3 A), suggesting the existence of HBsAg-specific cells in GKO rather than WT mice. Interestingly, the cotransfer of mixed splenocytes from HBV-carrier WT and GKO mice did

Figure 1. **IFN–γ maintains systemic tolerance during HBV persistence.** (A and B) 1 wk after HBV plasmid injection, WT, IFN–γ$^{-/-}$ (GKO), or IFN–γR1$^{-/-}$ (GRKO) mice were immunized with the HBsAg vaccine or PBS/Alum (vehicle) at weeks 0 and 2. Serum HBsAg levels were monitored weekly in the WT (A) or GKO (B) groups. The detection threshold for HBsAg is 2.0 ng/ml. (C) The percentage of serum HBsAg–positive mice was monitored. (D) Serum anti–HBs levels were monitored in all groups. (E and F) Fas$^+$GL7$^+$ GC B cells (gated on B220$^+$CD19$^+$ cells; E) and PD-1$^+$CXCR5$^+$ follicular helper T cells (Tfh; gated on CD4$^+$ T cells; F) were identified in draining lymph nodes (dLNs) and spleens of HBV-injected WT or GKO mice 8 d after the first vaccination or vehicle treatment. Representative flow cytometric plots are shown; the numbers inside indicate the percentages. (G and H) Serum HBeAg levels (G) and HBV DNA titers (H) were detected at week 3. NCU, national clinical units. (I) Splenocytes were isolated at week 3 and cultured for 3 d with or without HBsAg, and proliferation was measured by [³H]TdR incorporation. (J and K) Serum HBsAg (J) and anti–HBs (K) levels were examined in HBV-injected GRKO mice that received HBsAg vaccine or vehicle control. (L) The frequency of Fas$^+$GL7$^+$ GC B cells was calculated in the WT and GRKO groups. (A, B, and D–L) Data are expressed as the means ± SEM (unpaired Student's *t* test), and experiments were repeated at least three times (*n* = 3–6 mice per group). (C) Pooled results from three independent experiments are shown. Statistics analysis was performed by unpaired Student's *t* test. *, P < 0.05; **, P < 0.01; ***, P < 0.001.

not reduce anti–HBs production compared with the transfer of GKO splenocytes alone (Fig. 3 A), thus both indicating that splenocytes from HBV-tolerant WT mice were insufficient to inhibit antigen–specific responses and further ruling out a role for inhibitory cells in this transfer system. Moreover, Rag1$^{-/-}$ mice reconstituted with hepatic lymphocytes from GKO–HBV mice showed much lower anti–HBs production compared with reconstitution with splenocytes from the same mice (Fig. 3 B), suggesting that functional HBsAg-specific clones preferentially accumulated in the periphery (e.g., spleen) but not in the liver of HBV-carrier GKO mice.

We next reported that the loss of functional antigen-specific CD4$^+$ T cells was the major reason for systemic tolerance because CD4$^{-/-}$ mice reconstituted with splenocytes from HBV-carrier WT mice produced greatly diminished antibodies after HBsAg vaccination (Fig. 3 C), but splenocytes

from HBV–carrier GKO mice remained competent to induce strong antibody responses in CD4$^{-/-}$ mice, indicating that HBsAg-specific CD4$^+$ T cells were retained in the spleens of HBV-carrier GKO mice (Fig. 3 C). This was further demonstrated using MHC–II tetramer staining, which showed that HBV-carrier GKO mice had much more HBsAg$_{126–138}$–specific CD4$^+$ T cells in the spleen than WT mice (Fig. 3, D and E). Notably, although HBV-carrier WT mice still had a frequency of HBsAg-specific CD4$^+$ T cells in the periphery similar to that of naive WT mice (Fig. 3 D), that frequency was insufficient to induce anti–HBs production, thus suggesting the functional tolerance of these remnant CD4$^+$ T cell clones. In accordance with this result, HBsAg-specific CD4$^+$ T cells in HBV-carrier WT mice showed no expansion after vaccination, which was in sharp contrast to cells from HBV-carrier GKO mice (Fig. 3, F and G). Collectively, these results
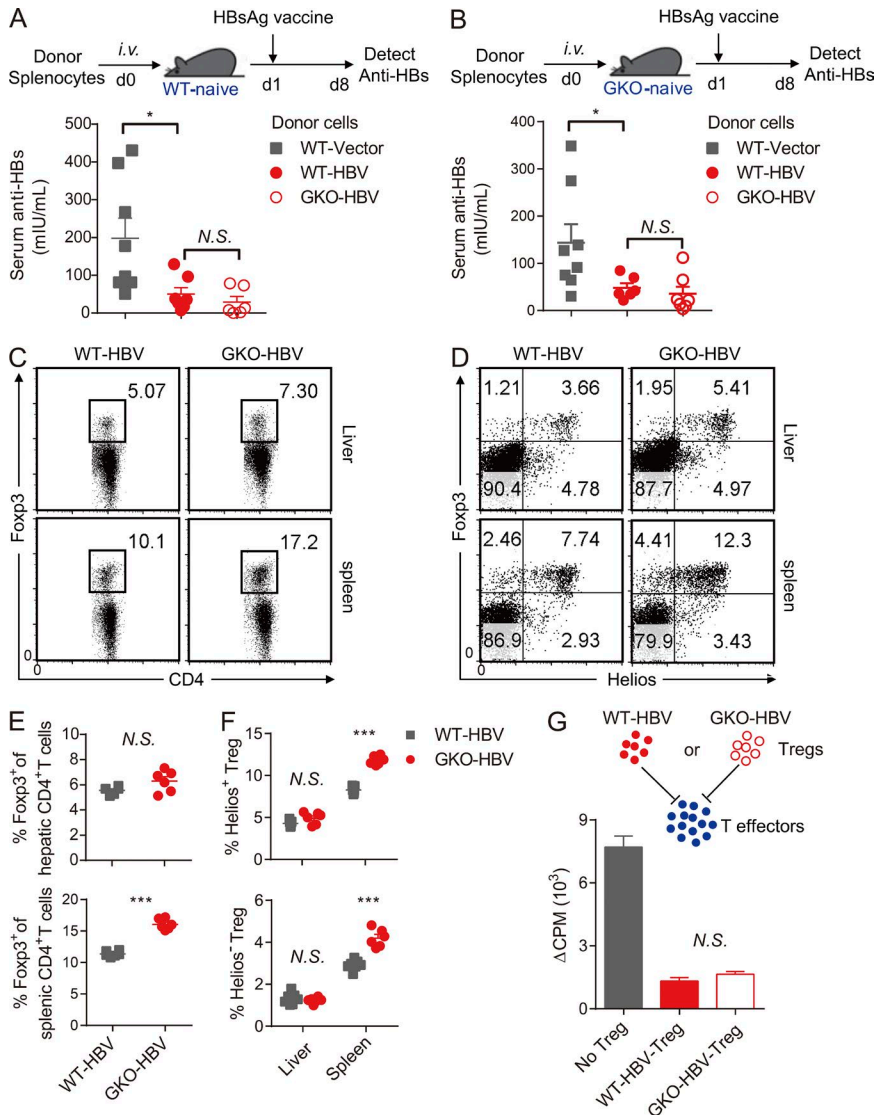
Figure 2. **IFN-γ–deficient mice exhibit intact inhibitory cells.** (A and B) Splenocytes from WT-vector, WT-HBV, or GKO-HBV mice were isolated 1 wk after HBV plasmid or control vector injection and transferred into naive WT (A) or naive GKO (B) mice. Recipients were subcutaneously immunized with HBsAg vaccine; serum anti-HBs levels were measured as depicted. (C–G) WT and GKO mice were injected with HBV plasmid. (C) 1 wk later, Foxp3 expression on hepatic (top) and splenic (bottom) CD4^{+} T cells in HBV-carrier WT or GKO mice was analyzed. (D) Foxp3 and Helios expression on hepatic (top) and splenic (bottom) CD4^{+} T cells was analyzed. (E and F) The frequencies of Foxp3^{+} cells (E) and Helios^{+}/Helios^{−} Foxp3^{+} cells (F) among CD4^{+} T cells were quantified. (G) WT CD4^{+}CD25^{−} effector T cells were cultured alone or cocultured with an equal number of CD4^{+}CD25^{+} T reg cells from either WT or GKO HBV-carrier mice in the presence of anti-CD3 plus anti-CD28, and proliferation was measured by [³H] TdR uptake. All data are expressed as the means ± SEM. (A and B) Representative results from two independent experiments with n = 5–7 per group are shown. One-way ANOVA followed by Bonferroni tests were applied. (C–G) Experiments were repeated twice with similar results; n = 5 mice per group. Unpaired Student's t test was used. *, P < 0.05; ***, P < 0.001.

indicated that the recovery of systemic responsiveness toward HBsAg vaccination in HBV-carrier GKO mice was caused by the conservation of functional HBsAg-specific CD4^{+} T cells in the periphery and that IFN-γ might play a critical role in supporting the clonal deletion/tolerance of antigen-specific CD4^{+} T cells during HBV persistence in the liver.

CD4^{+} T cells are the major producers of IFN-γ for the maintenance of tolerance

We next examined which immune cells provided IFN-γ to support tolerance. Depletion of NK1.1-positive cells (including NK and NKT cells) was insufficient to overcome HBV-induced systemic tolerance in this model (unpublished data), prompting us to examine the role of T cell–derived IFN-γ during HBV persistence. Interestingly, upon TCR restimulation, only hepatic-derived lymphocytes displayed enhanced IFN-γ production both after HBV injection and throughout the HBV-persistent period (Fig. 4, A and B). Moreover,

the enhanced IFN-γ production by hepatic T cells was absent after the injection of HBV e/core–null plasmid but neither HBeAg mutant nor HBsAg mutant plasmid (Fig. 4 C), suggesting that an HBV core antigen (HBcAg)–dependent manner was required for HBV-induced IFN-γ production. Indeed, HBcAg but not HBsAg restimulation was able to trigger IFN-γ production by hepatic-derived lymphocytes (Fig. 4 D). Specifically, hepatic CD4^{+} T cells were the dominant IFN-γ producers during HBV persistence (Fig. 4 E), whereas their production of IL-4 and TNF was not prominently affected, and the production of IL-2 significantly decreased (Fig. 4 F). Although IL-17A production by hepatic CD4^{+} T cells was increased (Fig. 4 F), HBV-carrier IL-17A^{−/−} mice only showed transient reduction of serum HBsAg and no reduction of HBeAg after HBsAg vaccination (Fig. 4, G and H). Additionally, their splenocytes were not able to reconstitute anti-HBs responses in CD4^{−/−} mice, indicating that IL-17A production was not essential for maintaining systemic tolerance (Fig. 4 I).
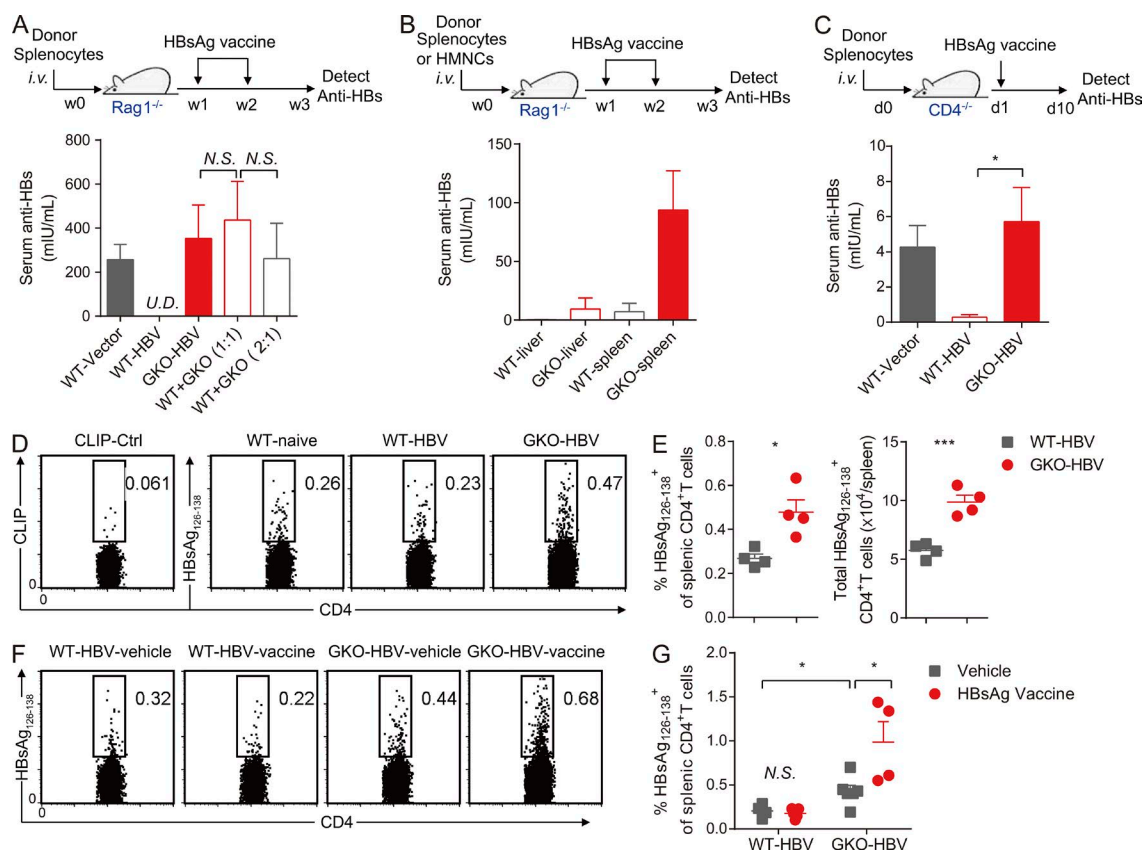
Figure 3. **IFN–γ deficiency leads to the preservation of functional HBsAg–specific CD4⁺ T cell clones in the periphery.** (A and C) Splenocytes from WT-vector, WT-HBV, or GKO-HBV mice were isolated 1 wk after plasmid injection and transferred into Rag1$^{-/-}$ (A) or CD4$^{-/-}$ mice (C). (B) 10^7 hepatic mononuclear cells (HMNCs) or splenocytes from WT-HBV or GKO-HBV mice were transferred into Rag1$^{-/-}$ mice. Recipient mice were subcutaneously immunized with HBsAg vaccine; serum anti-HBs levels were measured as depicted. (D and E) The percentage and absolute numbers of HBsAg$_{126-138}$-specific CD4$^+$ T cells in the spleens of WT or GKO mice are shown 1 wk after HBV plasmid injection. (F and G) HBV-carrier WT or GKO mice were immunized with HBsAg vaccines or vehicles twice at 2-wk intervals. The frequencies of splenic HBsAg$_{126-138}$-specific CD4$^+$ T cells were examined 1 wk after the last vaccination. Data represent the means ± SEM for three to five mice per group. Experiments were repeated at least four times for A and C and at least two times for B and D–G. Statistical analysis was performed by unpaired Student's t test. U.D., undetectable. *, $P < 0.05$; ***, $P < 0.001$.

To formally test the requirement for CD4$^+$ T cell–derived IFN–γ in the maintenance of peripheral tolerance to HBV, CD4$^{-/-}$ mice were reconstituted with WT, GKO, or GRKO CD4$^+$ T cells (Fig. 4, J and K) to generate HBV-persistent mice with IFN–γ or IFN–γ receptor deficiency in CD4$^+$ T cells only. We found that only splenocytes from CD4$^{-/-}$ mice reconstituted with GKO CD4$^+$ T cells successfully elicited HBsAg-specific immunity in HBV-vaccinated Rag1$^{-/-}$ mice (Fig. 4 L), further suggesting a distinct role for CD4$^+$ T cell–derived IFN–γ in maintaining tolerance. Importantly, splenocytes from HBV-carrier CD4$^{-/-}$ mice reconstituted with GRKO CD4$^+$ T cells maintained tolerance toward HBsAg, suggesting that IFN–γ exerted its tolerogenic effect in a paracrine rather than an autocrine manner (Fig. 4 L).

The CXCL9–CXCR3 pathway chemoattracts T cells to the liver to maintain tolerance

We proposed that decreased numbers of HBsAg-specific CD4$^+$ T cells in the periphery of WT-HBV mice should be caused by either increased T cell death/tolerization or increased T cell retention in the liver. Given the fact that IFN–γ acts in a paracrine manner during HBV persistence, we hypothesized that IFN–γ might induce the expression of either a death- or an inhibition-related ligand. To test this hypothesis, we detected several IFN–γ–regulated genes that have been reported to promote T cell apoptosis/inactivation, including *inos*, *ido*, *fasl* (ligand of Fas), *pdl1* (ligand of PD1), and *gal9* (ligand of Tim3); excluding programmed death ligand 1 (PD-L1), the mRNA expression of these genes in liver tissues from HBV-persistent WT mice or GRKO mice was comparable (Fig. 5 A). However, PD-L1 overexpression in the liver of GRKO-HBV mice was not able to restore the tolerance (Fig. 5 B). Additionally, blockade of PD-L1 in WT-HBV mice failed to recapitulate the phenotype of GRKO-HBV mice (Fig. 5 C), and it is thus not likely that IFN–γ maintains systemic tolerance via promoting PD-L1 expression.

T cell retention in the liver has been recognized as the fundamental basis for systemic T cell clone deletion (Crispe et
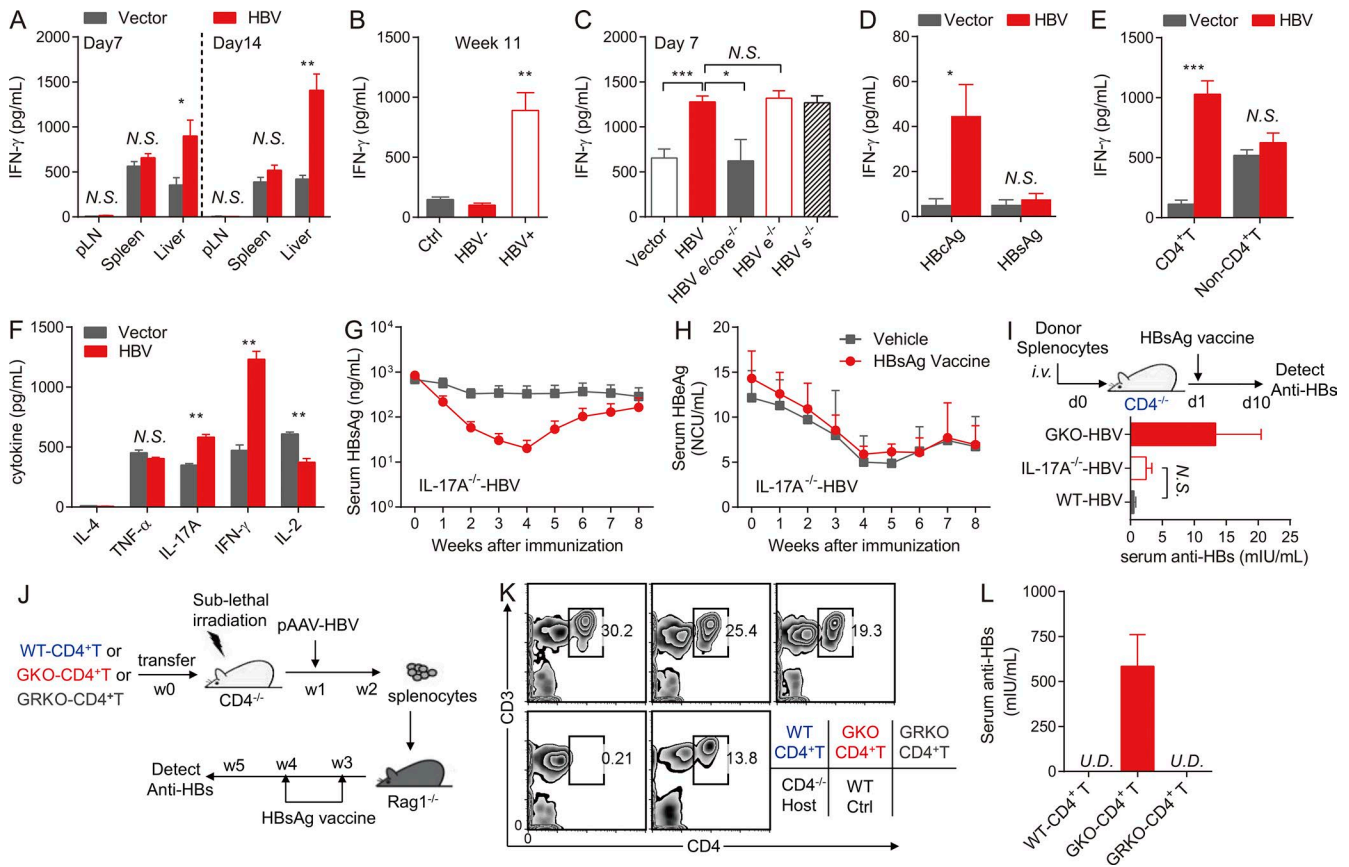
Figure 4. CD4+ T cells are the major producers of IFN-γ for the maintenance of tolerance. (A) Mononuclear cells from different organs were isolated 1 or 2 wk after HBV plasmid injection and restimulated in vitro to evaluate IFN-γ production. (B) Mice were categorized as HBV+ (serum HBsAg > 200 ng/ml), HBV− (serum HBsAg < 2 ng/ml), or Ctrl (control plasmid) at 11 wk after HBV plasmid injection. Hepatic mononuclear cells were then isolated and restimulated to evaluate IFN-γ production. (C) Mice were injected with pAAV control plasmid, pAAV-HBV plasmid, or eAg/cAg–deficient, e antigen–deficient, or s antigen–deficient HBV plasmid, and hepatic mononuclear cells were isolated 1 wk later and restimulated to evaluate IFN-γ production. (D) Hepatic mononuclear cells were isolated 1 wk after HBV plasmid injection and restimulated with HBcAg or HBsAg to evaluate IFN-γ production. (E) Hepatic CD4+ T and CD4+ T cell–depleted (Non-CD4+ T) cells were separated 1 wk after HBV plasmid injection and restimulated to evaluate IFN-γ production. (F) Hepatic CD4+ T cells were separated 1 wk after HBV or control plasmid injection and restimulated to evaluate IL-4, TNF, IL-17A, IFN-γ, and IL-2 production. (G and H) 1 wk after HBV plasmid injection, IL-17A−/− mice were immunized with HBsAg vaccine or PBS/Alum (vehicle) at week 0 and 2. Serum HBsAg (G) and HBeAg (H) levels were monitored weekly. NCU, national clinical units. (I) CD4−/− mice were transferred with the indicated splenocytes and immunized with HBsAg vaccine; anti-HBs levels were measured. (J and L) Sublethally irradiated CD4−/− mice reconstituted with the indicated CD4+ T cells were injected with HBV plasmid, and their splenocytes were used to reconstitute Rag1−/− mice (J), and anti-HBs levels in reconstituted Rag1−/− were measured after vaccination (L). (K) The efficiency of reconstituting the CD4+ T population in the peripheral blood of recipient CD4−/− mice was evaluated 1 wk after transfer. The peripheral blood of CD4−/− and WT host mice were used as controls. (A–F) Data were pooled from three to four mice per group. All the graphs show the means ± SEM from at least two independent experiments. (G and H) n = 5 mice per group. (I–L) n = 3 mice per group. Statistical analysis was performed by unpaired Student's t test. U.D., undetectable. *, P < 0.05; **, P < 0.01; ***, P < 0.001.

al., 2000; Mehal et al., 2001; von Oppen et al., 2009); therefore, we also compared the expression of several IFN-γ–regulated adherent genes in livers from HBV-persistent WT and GRKO mice, including *icam1, vcam1, cxcl9, cxcl10,* and *cxcl11.* We found that *cxcl9,* a T cell chemoattractant, was significantly down-regulated in HBV-carrier GRKO mice, both at mRNA (Fig. 5 A) and protein levels (Fig. 5 D). Consistent with this finding, CD49dhiCD11ahiCD4+ T cells, which have been reported to represent the HBV-primed CD4+ T cells in this HBV-persistent model (McDermott and Varga, 2011;

Zeng et al., 2013), and tetramer-labeled HBsAg126–138–specific CD4+ T cells were accumulated in the livers of HBV-carrier WT mice but not in GRKO mice (Fig. 5, E–H). Interestingly, the hepatic influx of HBsAg-specific CD4+ T cells occurred prominently ∼1–2 wk after HBV injection (Fig. 5 I), coinciding with the time course when the systemic tolerance was established (Xu et al., 2014). The accumulation of WT HBV-specific CD4+ T cells in the liver was the result of selective retention rather than in situ activation of T cells because the distribution of transferred CD45.1+CD49dhiCD11ahiCD4+
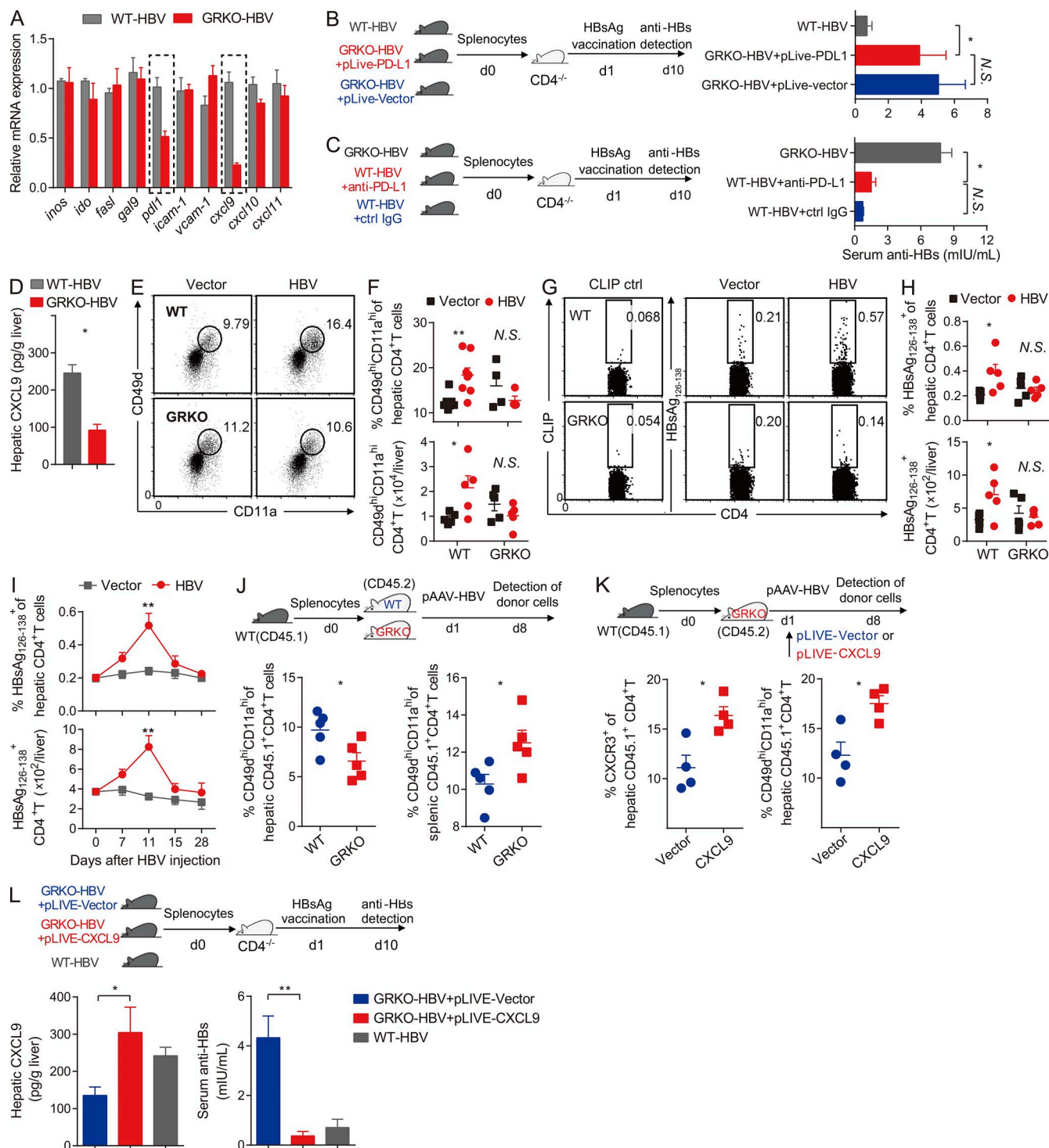
Figure 5. **CXCL9 chemoattracts T cells into the liver to maintain tolerance.** (A) Real-time PCR of genes in the liver from WT or GRKO HBV-carrier mice 1 wk after HBV plasmid injection. (B) Splenocytes from GRKO mice simultaneously injected with HBV plasmid and PD-L1–expressing plasmid or control vector were adoptively transferred to reconstitute the CD4$^{-/-}$ mice, as depicted. The anti-HBs levels in recipients were measured. (C) Splenocytes from WT-HBV mice treated with anti–PD-L1 or control IgG (ctrl IgG) were adoptively transferred to reconstitute CD4$^{-/-}$ mice as depicted, and the anti-HBs levels were measured. (D) CXCL9 protein levels in liver tissue homogenates of HBV-carrier WT or GRKO mice. (E–H) WT or GRKO mice were injected with HBV or control plasmid, and hepatic mononuclear cells were isolated 10 d later. Percentages and total numbers of hepatic CD49d^{hi}CD11a^{hi} cells (gated on CD3$^+$NK1.1$^-$CD4$^+$ T cells; E and F) and of HBsAg$_{126–138}$-specific CD4$^+$ T cells (G and H) were detected by flow cytometry. (I) WT mice were injected with HBV or control plasmid, and hepatic mononuclear cells were isolated at the indicated time points for detection of the frequencies and total numbers of HBsAg$_{126–138}$-specific CD4$^+$ T

T cells increased in the liver but decreased in the spleen of HBV-carrier WT mice compared with HBV-carrier GRKO mice (Fig. 5 J). We speculated that this result might help explain the loss of tolerance to HBV persistence in the absence of IFN-γ signaling: a diminished hepatic recruitment of the HBV-responsive CD4$^+$ T cells of GRKO mice might prevent the functional deletion of these T cells in the liver. Thus, we predicted that increased CXCL9 production could enhance T cell retention in the liver and restore HBV tolerance in GRKO mice. Indeed, liver-targeted CXCL9 overexpression restored the retention of CXCR3$^+$CD4$^+$ (CXCR3 is the receptor for CXCL9) or CD49d^{hi}CD11a^{hi}CD4$^+$ T cells in the livers of HBV-carrier GRKO mice (Fig. 5 K). More importantly, CXCL9 overexpression dramatically reduced HBsAg-specific CD4$^+$ T cells in the spleen and thus failed to reconstitute HBsAg-specific immune responses in CD4$^{-/-}$ mice (Fig. 5 L), indicating that CXCL9-mediated migration of HBV-specific T cells into the liver was sufficient to recover HBV-induced systemic tolerance. It is worth noting that hepatic CXCL9 levels in liver-targeted CXCL9 overexpressed GRKO-HBV mice were comparable with WT-HBV mice (Fig. 5 L, left), suggesting that restoration of CXCL9 to the levels of WT-HBV mice is sufficient to maintain the systemic tolerance.

Consistent with the critical role of CXCL9 in the hepatic retention of HBV-specific CD4$^+$ T cells, HBV-specific CD49d^{hi}CD11a^{hi}CD4$^+$ T cells selectively expressed high levels of CXCR3 (Fig. 6 A). The frequencies of CXCR3$^+$CD4$^+$ T cells or CXCR3$^+$ HBsAg$_{126–138}$–specific CD4$^+$ T cells were also significantly enhanced after HBV challenge (Fig. 6, B–D), further supporting a contribution of the CXCR3–CXCL9 pathway to tolerance during HBV persistence. As expected, antibody blockade of CXCR3 abrogated liver homing of CD49d^{hi}CD11a^{hi}CD4$^+$ T cells or HBsAg$_{126–138}$–specific CD4$^+$ T cells in HBV-carrier WT mice (Fig. 6 E). Furthermore, splenocytes from CXCR3-blocked HBV-carrier WT mice partially reconstituted HBsAg-specific immunity in CD4$^{-/-}$ mice (Fig. 6 F), indicating that the blockade of CXCR3 could reverse HBV-induced systemic tolerance by attenuating the hepatic retention of CD4$^+$ T cells.

Liver–resident macrophages contribute to T cell retention and tolerance

To pinpoint the IFN-γR–bearing cell required for inducing tolerance to HBV, we next sought to identify the hepatic CXCL9-producing cell type. Both hepatocytes and liver nonparenchymal cells (LNPCs) from HBV-carrier GRKO mice produced less CXCL9 than those from WT mice;

however, HBV prompted CXCL9 production only from WT LNPCs (Fig. 7 A) and specifically from F4/80$^+$ cells (Fig. 7 B), creating the possibility that liver-resident macrophages (Kupffer cells) produced CXCL9 in response to CD4$^+$ T cell–derived IFN-γ stimulation during HBV persistence. To confirm this, Kupffer cells were depleted in vivo by clodronate liposome treatment before HBV injection (Fig. 7 C). Indeed, HBV-induced hepatic CXCL9 up-regulation, CD49d^{hi}CD11a^{hi}CD4$^+$ T cell infiltration, and CXCR3$^+$ T cell retention were abolished, as expected (Fig. 7, D–F). Consistent with this finding, splenocytes from Kupffer cell–depleted HBV-injected mice reconstituted HBsAg-specific immunity in CD4$^{-/-}$ mice (Fig. 7 G), indicating that HBV-induced systemic tolerance was lost in the absence of Kupffer cells. However, hepatic ectopic expression of CXCL9 could partially restore the tolerance in Kupffer cell–depleted HBV mice, suggesting that Kupffer cells contribute to tolerance at least partially through CXCL9-mediated hepatic retention of T cells. In addition, we assessed the frequency of HBV-primed CD11a^{hi}CD8α^{lo}CD8$^+$ T cells (Zeng et al., 2013), and we found that Kupffer cells also promoted the hepatic accumulation of HBV-primed CD8$^+$ T cells or CXCR3$^+$CD8$^+$ T cells (Fig. 7, H–J), implicating the central role of Kupffer cells in the chemoattraction of antigen-experienced T cells during HBV persistence in the liver.

Apoptosis of hepatic HBsAg–specific CD4$^+$ T cells is associated with systemic tolerance

We sought to explore the mechanisms underlying the tolerization of liver-retained HBsAg-specific CD4$^+$ T cells. Intrahepatic HBsAg-specific CD4$^+$ T cells exhibited a high expression level of the apoptotic marker annexin V (Fig. 8 A). Moreover, annexin V–positive HBsAg$_{126–138}$ CD4$^+$ T cells were significantly increased in the livers of tolerized WT mice but not GRKO mice (Fig. 8 B), indicating that the apoptosis of HBsAg-specific CD4$^+$ T cells was associated with systemic tolerance against HBsAg vaccination. Coinhibitory receptors were considered the principal mediators of T cell tolerization during chronic hepatitis virus infection, promoting intrahepatic T cell dysfunction or apoptotic deletion (Maini and Schurich, 2010; Schurich et al., 2011; Nebbia et al., 2012). We assessed the expression of the coinhibitory receptor CTLA-4, PD-1, TIM-3, and LAG-3 on intrahepatic HBsAg$_{126–138}$ CD4$^+$ T cells of HBV-carrier WT mice 1 wk after HBV challenge, when systemic tolerance was establishing. A significant increase in CTLA-4 expression was observed, whereas no obvious changes in PD-1, TIM-3, or LAG-3 were identified in

cells. (J) Splenocytes from naive CD45.1$^+$ mice were transferred into WT or GRKO recipients as depicted, and the distribution of donor CD49d^{hi}CD11a^{hi}CD4$^+$ T cells (CD45.1$^+$) in livers and spleens of CD45.2$^+$ recipients was analyzed 8 d after HBV plasmid injection. (K) Donor CXCR3$^+$CD4$^+$ (left) and CD49d^{hi}CD11a^{hi}CD4$^+$ (right) T cell distribution in livers of CXCL9-expressing or empty plasmid–injected GRKO-HBV mice. (L) Splenocytes from GRKO mice simultaneously injected with HBV plasmid and CXCL9-expressing plasmid or control vectors were isolated after 1 wk to reconstitute the CD4$^{-/-}$ mice; CXCL9 protein levels in liver tissue homogenates of donor mice (left) and anti-HBs levels in recipient CD4$^{-/-}$ mice (right) were measured. Data are shown as the means ± SEM. Results are representative of at least two independent experiments (n = 3–6 mice per group). Unpaired Student's t test was used. *, P < 0.05; **, P < 0.01.

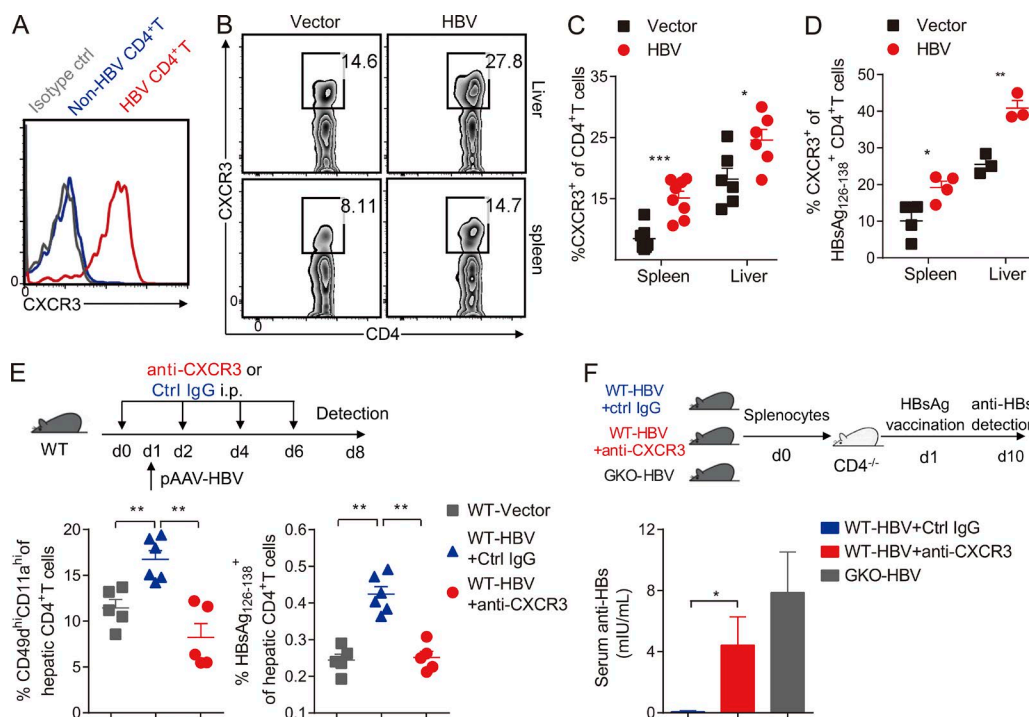IFN-γ maintains liver-induced systemic tolerance | Zeng et al.

Figure 6. Blockade of CXCR3 partially reverses HBV-induced systemic tolerance. (A) WT mice were injected with HBV plasmid, and the expression of CXCR3 on hepatic CD49d^{hi}CD11a^{hi}CD4$^+$ T cells (HBV CD4$^+$T) or CD49d^{lo}CD11a^{lo}CD4$^+$ T cells (Non-HBV CD4$^+$ T) after 1 wk is shown. (B–D) The CXCR3$^+$ cell frequency in CD3$^+$NK1.1$^-$CD4$^+$ T cells (B and C) and in HBsAg$_{126-138}$-specific CD4$^+$ T cells (D) of WT-HBV or control (ctrl) mice is shown. (E) WT-HBV mice were treated with anti-CXCR3 or ctrl IgG as depicted, and frequencies of hepatic CD49d^{hi}CD11a^{hi} T cells (left) or HBsAg$_{126-138}$-specific CD4$^+$ T cells (gated on 7-AAD$^-$CD3$^+$NK1.1$^-$ CD4$^+$ cells; right) are shown. (F) The indicated splenocytes were transferred into CD4$^{-/-}$ mice 1 wk after HBV injection (2 d after the last antibody treatment); anti-HBs levels were measured in recipient mice. Reconstitution with splenocytes from GKO-HBV mice served as the positive control. (A–D) Results are representative of three independent experiments. (E and F) Experiments were repeated twice with similar results. Data are expressed as means ± SEM (n = 3–6 per group). Statistical analysis was performed by Student's *t* test. *, P < 0.05; **, P < 0.01; ***, P < 0.001.

the tolerized mice compared with the control vector–injected mice (Fig. 8 C). Antibody blockade of CTLA-4 could significantly prevent the apoptosis of HBsAg-specific T cells in the liver and increase their numbers in the spleen (Fig. 8 D), suggesting a proapoptotic role for CTLA-4 in the intrahepatic elimination of HBsAg-specific CD4$^+$ T cells. Notably, splenocytes from CTLA-4–blocked WT-HBV mice successfully reconstituted HBsAg-specific immunity in CD4$^{-/-}$ mice, leading to enhanced anti-HBs production after vaccination in these adaptive immune-deficient mice (Fig. 8 E), which suggests that the blockade of CTLA-4 could partially reverse HBV-induced systemic tolerance. Additionally, consistent with previous studies that IL-2 deprivation was implicated in CTLA-4–mediated T cell inhibition (Wing et al., 2011), hepatic CD4$^+$ T cells in tolerized mice showed impaired production of IL-2 (Fig. 4 F). Moreover, the administration of IL-2 reduced the hepatic apoptosis of HBsAg-specific CD4$^+$ T cells, increased their numbers in the spleen, and reversed the systemic tolerance (Fig. 8, F and G).

Finally, to assess if the recovery of systemic HBsAg-specific CD4$^+$ T cells by CTLA-4 blockade or IL-2 supplement had therapeutic potentials against established HBV infection,

HBV-carrier mice were treated with anti–CTLA-4, IL-2, or both, followed by HBsAg vaccination (Fig. 9 A). We found that HBV-carrier mice receiving combination therapy with anti–CTLA-4 and HBsAg vaccine exhibited dramatically decreased serum levels of HBsAg, HBeAg, and HBV DNA (Fig. 9, B–D) and detectable anti-HBs titers (Fig. 9 E). However, IL-2 showed poor therapeutic effects when combined with the vaccine and had no synergistic effect with anti–CTLA-4 (Fig. 9, B–E). Collectively, these data highlight a role of CTLA-4 in contributing to the HBV persistence–induced systemic tolerance, and anti–CTLA-4 could be a potential adjuvant for designing therapeutic vaccines against CHB.

DISCUSSION

In this study, we revealed the dual roles played by IFN-γ during liver viral antigen persistence. On the one hand, IFN-γ was critical for viral clearance because a deficiency in IFN-γ hindered spontaneous HBV elimination and promoted HBV persistence (Fig. 1 C). On the other hand, IFN-γ was critical for maintaining liver tolerance because IFN-γ deficiency abolished HBV persistence–induced systemic tolerance and restored immune responses to peripheral HBV vaccination
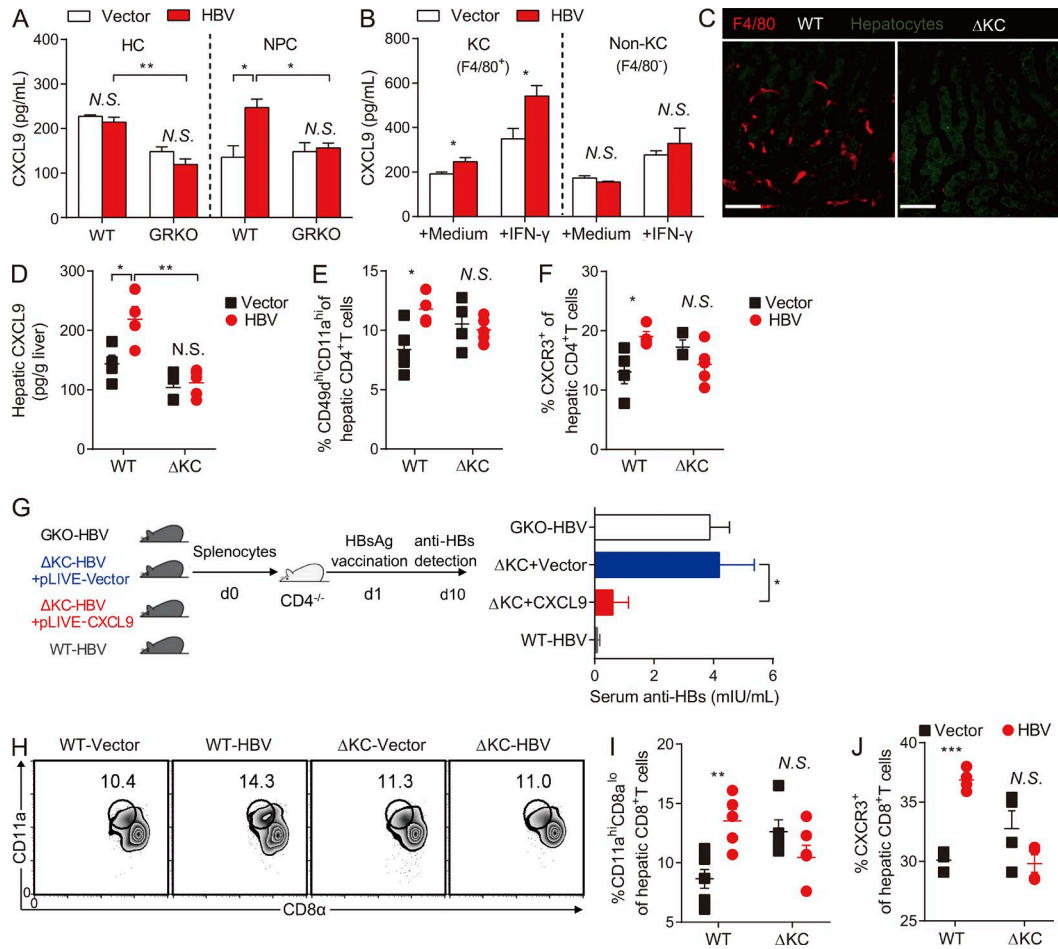
Figure 7.   **Liver–resident macrophages contribute to T cell retention and tolerance.** (A and B) 1 wk after HBV plasmid injection, hepatocytes (HC; A, left) and LNPCs (A, right) from WT and GRKO mice or F4/80$^+$ (Kupffer cells [KC]) and F4/80$^-$ LNPCs from WT mice (B) were sorted and cultured in vitro, and CXCL9 levels in the supernatant were measured. (C) WT mice were treated with clodronate liposomes (ΔKC) or control liposomes ("WT") 1 d before HBV or control plasmid injection, and the depletion efficiency was verified by immunofluorescence staining of F4/80 (red) on liver tissue sections. Bars, 30 μm. (D–F) 8 d later, CXCL9 levels in liver tissue homogenates were measured, and the frequency of CD49d^{hi}CD11a^{hi} (E) and CXCR3$^+$ cells among CD4$^+$ (F) T cells in the liver were detected. (G) Kupffer cell–depleted mice were simultaneously injected with HBV plasmid and CXCL9-expressing plasmid or control vectors; 1 wk later, splenocytes were harvested to reconstitute CD4$^+$ T immunity in CD4$^{-/-}$ mice, and anti-HBs levels were measured. Reconstitution with splenocytes derived from WT- or GKO-HBV mice was set as the negative or positive control, respectively. (H–J) WT-HBV mice were treated with clodronate liposomes or control liposomes. The frequency of CD11a^{hi}CD8a^{low} (H and I) and CXCR3$^+$ (J) cells among CD8$^+$ T cells in the liver was detected at day 8. All graphs show the means ± SEM from at least two independent experiments (n = 3–5 mice per group). Pooled cells from three mice per group are shown in A and B. Statistical analysis was performed by Student's t test analysis. *, P < 0.05; **, P < 0.01; ***, P < 0.001.

(Fig. 1). Recent studies indicate that chronic lymphocytic choriomeningitis virus infection can redirect IFN-α/β to induce negative immunity to support viral persistence instead of clearance (Teijaro et al., 2013; Wilson et al., 2013). Similarly, we demonstrated here that IFN-γ can also be hijacked to support viral immune evasion in our HBV persistence model. This tolerogenic role of IFN-γ revealed herein has several clinical implications. For example, one of the gold standards for evaluating the efficiency of a therapeutic vaccine against HBV is the IFN-γ–producing ability of T cells. Based on our findings that antigen-stimulated moderate/chronic IFN-γ production promotes systemic tolerance, this gold standard might need to

be carefully reconsidered, especially in cases lacking a strong immune adjuvant. Consistent with this, evidence from clinical trials has indicated that elevated production of IFN-γ by T cells is not always coupled with improved control of HBV during vaccine therapy (Jung et al., 2002), presumably because moderate IFN-γ production could strengthen systemic tolerance to vaccines in patients with CHB.

Two prevalent mechanisms, including the induction of antigen-specific inhibitory cells and the deletion/anergy of antigen-specific T cells, are responsible for liver-induced systemic tolerance in various models (Mehal et al., 2001; Dobrzynski et al., 2004; Dong et al., 2004; Cao et al., 2007;
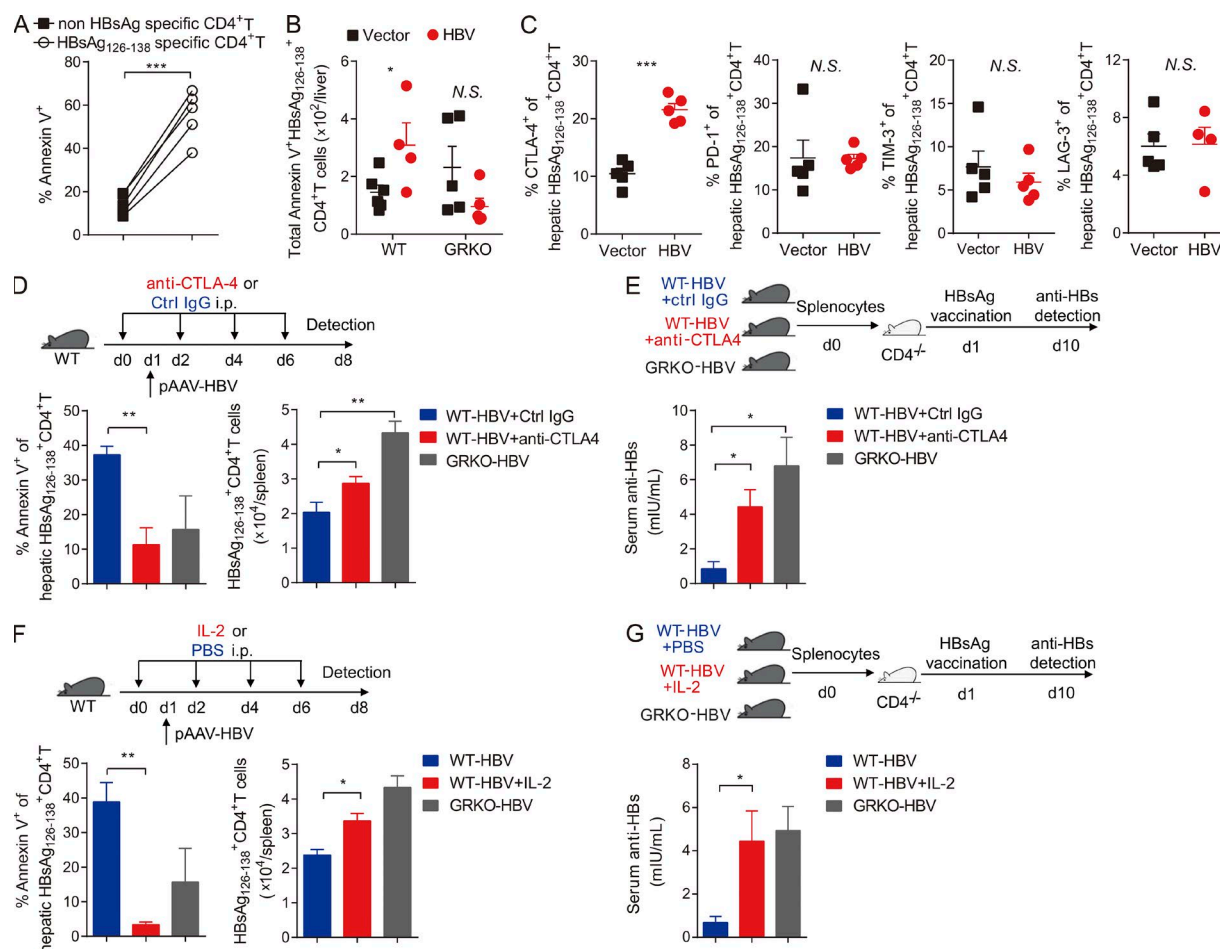
Figure 8. Apoptosis of hepatic HBsAg–specific CD4⁺ T cells is associated with systemic tolerance. (A) The expression levels of annexin V on HBsAg$_{126-138}$-specific or nonspecific CD4⁺ T cells from WT-HBV mice were compared. (B) The total number of annexin V–positive HBsAg$_{126-138}$-specific CD4⁺ T cells in the livers of WT or GRKO mice 1 wk after HBV or control plasmid injection is shown. (C) Expression of CTLA-4, PD-1, Tim-3, and Lag-3 on hepatic HBsAg$_{126-138}$-specific CD4⁺ T cells 1 wk after HBV plasmid injection. (D and E) WT-HBV mice were treated with anti-CTLA-4 or control IgG (ctrl IgG) as depicted. (D) The frequency of annexin V⁺ HBsAg$_{126-138}$-specific CD4⁺ T cells in the liver (left) or the total number of HBsAg$_{126-138}$-specific CD4⁺ T cells in the spleen (right) is shown. (E) CD4⁻/⁻ mice were reconstituted with the indicated splenocytes (splenocytes were isolated 2 d after the last antibody treatment) and then immunized with HBsAg vaccine. Serum anti-HBs levels were measured. (F and G) WT-HBV mice were injected with rIL-2 (25,000 U) or PBS every other day for four times as depicted. (F) The frequency of annexin V–positive HBsAg tetramer⁺ CD4⁺ T cells in liver (left) and total numbers of HBsAg$_{128-136}$ tetramer⁺ CD4⁺ T cells in the spleen (right) were detected. (G) Splenocytes from IL-2– or PBS-treated WT-HBV mice were isolated and reconstituted CD4⁻/⁻ mice as depicted; anti-HBs levels were measured. Data are expressed as means ± SEM with $n = 5$ mice per group in A–C and $n = 3$–5 mice per group in D–G. Representative results from two independent experiments are shown. Statistical analysis was performed by Student's t test (paired for A, unpaired for the rest). *, $P < 0.05$; **, $P < 0.01$; ***, $P < 0.001$.

Lüth et al., 2008; Breous et al., 2009; von Oppen et al., 2009). Here, we confirmed that both mechanisms occurred in our HBV tolerance model. Whereas HBV-carrier GKO and WT mice both exhibited intact antigen-specific inhibitory cells (Fig. 2), HBV-carrier GKO mice retained more functional T cell clones in the periphery than HBV-carrier WT mice, leading to a loss of tolerance in HBV-carrier GKO mice during the recall response (Fig. 3). In this regard, T cell clonal deletion/anergy seems to be more powerful than antigen-specific inhibitory cells in determining systemic tolerance during a persistent viral state, although the contribution of each mechanism at various times during viral persistence and in different organs must be further investigated.

Liver-induced systemic tolerance in our model required 7–10 d to establish and lasted throughout HBV persistence (Xu et al., 2014), coinciding with the kinetics of HBV-triggered IFN-γ production (Fig. 4). We supposed that the initial production of IFN-γ was mediated by intrahepatic TCR activation, which was likely dependent on the HBcAg based both on our findings (Fig. 4, C and D) and on those of another study using plasmids to knock out HBcAg expression (Lin et al., 2010). Moreover, this TCR activation imprinted
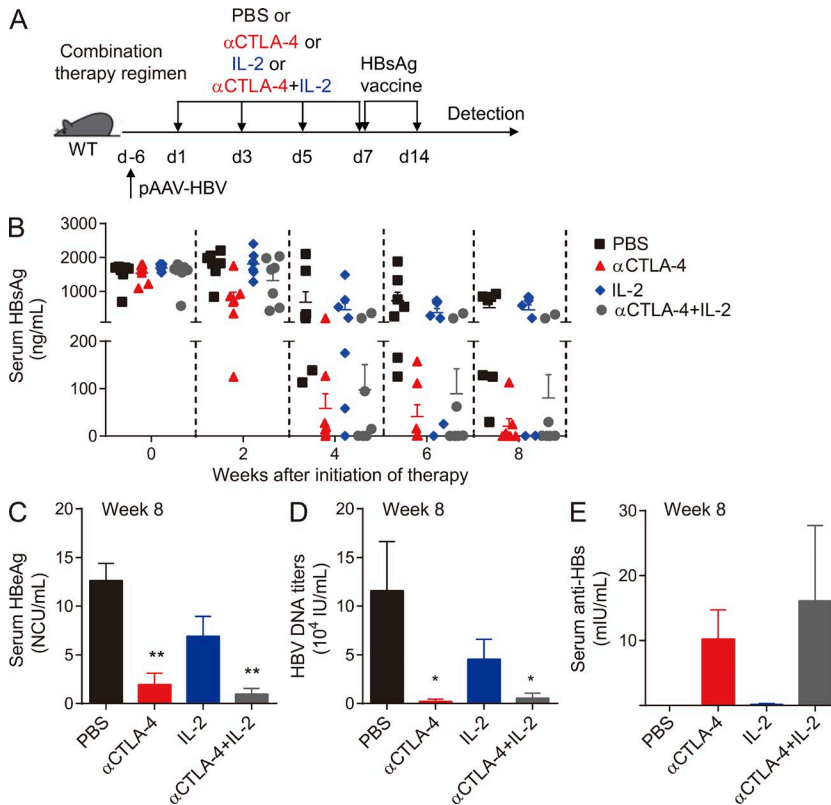
Figure 9. **Anti–CTLA-4 efficiently improves therapeutic vaccination against HBV.** (A) 1 wk after HBV plasmid injection, WT-HBV mice were treated with anti–CTLA-4, IL-2, or both, followed by HBsAg vaccination as depicted (termed as combination therapy regimen). (B) Serum HBsAg levels were monitored in all groups weekly. (C–E) Serum HBeAg levels (C), HBV DNA titers (D), and anti-HBs levels (E) were detected at week 8 after the initiation of treatment. NCU, national clinical units. One of two independent experiments is shown (n = 5–7 mice per group). Data are expressed as means ± SEM. Statistical analysis was performed by Student's t test. *, P < 0.05; **, P < 0.01.

an unusual cytokine profile onto CD4$^+$ T cells, which was similar to Th1 but lacked TNF up-regulation and displayed reduced IL-2 production (Fig. 4 F). This special T cell differentiation pattern was possibly affected by the cytokine milieu associated with liver tolerance, such as increased IL-10 production by Kupffer cells after HBV challenge (Xu et al., 2014). The enhanced IL-17A production observed herein may have been derived from intrahepatic CD4$^+$γδ T cells, which have previously been reported to be the major IL-17A producers during HBV persistence. IL-17A deficiency leads to an impaired recruitment of myeloid-derived suppressor cells (Kong et al., 2014); this could explain why transient and limited immune responses against HBsAg vaccination were evoked in IL-17A$^{-/-}$ HBV-carrier mice (Fig. 4, G–I).

The IFN-γ–stimulated immune regulators involved in maintaining systemic tolerance were investigated. Although IFN-γ partially regulated PD-L1 expression (Fig. 5 A) and the PD-1–PD-L1 interaction promoted T cell tolerance in our model (Tzeng et al., 2012), PD-L1 is not likely coupled with IFN-γ in maintaining systemic T cell tolerance that begins at an early phase of HBV persistence (Fig. 5, B and C). Instead, the PD-1–PD-L1 axis usually promotes T cell exhaustion at the late phase of viral persistence. In support of this, PD-1 up-regulation on T cells was not observed until at least 3–4 wk after the onset of HBV persistence in our model (Tzeng et al., 2012). We eventually found that IFN-γ–stimulated hepatic CXCL9 expression was involved in maintaining systemic tolerance. However, the opposite

conclusion was reached in a study showing that CXCR3–CXCL9-mediated hepatic trafficking of T cells gave rise to immunity rather than tolerance after polyinosinic:polycytidylic acid stimulation in mice with transgenic lymphocytic choriomeningitis virus expression in the liver (Lang et al., 2006). We think that this divergent outcome may be caused by the different inflammation conditions associated with each model. The inflammatory state assessed in our model was very weak and long lasting; the viral antigen–stimulated IFN-γ response in our model was moderate and elicited a mild up-regulation of chemokine expression. However, it would be interesting to distinguish between the roles of antigen- and inflammation–driven chemotaxis during viral persistence.

We proposed that hepatic trapped antigen-specific CD4$^+$ T cells may undergo apoptotic deletion/inactivation to finally maintain systemic tolerance. This was supported by evidence demonstrating increased numbers of intrahepatic apoptotic HBsAg-specific CD4$^+$ T cells in tolerized WT but not GRKO mice. CTLA-4 ligation was involved in intrahepatic apoptotic deletion because CTLA-4 blockade dramatically reduced apoptosis and reversed systemic tolerance (Fig. 8). A previous study showed that CTLA-4 was preferentially up-regulated on Bim-expressing apoptosis-prone HBV-specific T cells and that abrogation of CTLA-4 signaling could reduce Bim expression (Schurich et al., 2011). Thus, it is reasonable to postulate that CTLA-4–delivered signals on

T cells (presumably by inhibiting IL-2 production) during chronic viral infection could initiate Bim–mediated apoptosis.

Overall, we identified an unexpected contribution of IFN-γ and its related CXCL9–CXCR3-mediated hepatic T cell retention in the maintenance of systemic tolerance in hosts with viral persistence in the liver. To our knowledge, this is the first study to explore the mechanism underlying the ability of viral persistence in the liver to induce systemic T cell tolerance; moreover, it might explain the development of CHB patients' paralysis related to peripheral HBV antigen vaccination. Thus, our study has great value not only for understanding the pathogenesis of viral diseases in the liver but also for the design of effective immunotherapeutic drugs.

MATERIALS AND METHODS

Mice. 6-wk-old male WT C57BL/6 mice were purchased from the Shanghai Experimental Animal Center. IFN-γ$^{-/-}$ (GKO), IFN-γR1$^{-/-}$ (GRKO), and Rag1$^{-/-}$ mice were purchased from the Model Animal Research Center. CD45.1^{+} mice were purchased from The Jackson Laboratory. CD4$^{-/-}$ mice were a gift from Z. Lian (University of Science and Technology of China, Hefei, China). IL-17A$^{-/-}$ mice were provided by Z. Yin (Nankai University, Tianjin, China). All mice were on a B6 background, maintained under specific pathogen–free conditions, and used in accordance with the National Institutes of Health Guide for the Care and Use of Laboratory Animals.

Plasmids. The pAAV vector and pAAV-HBV1.2, pAAV-HBV1.2-e/core–null, pAAV-HBV1.2-e–null, and pAAV-HBV1.2-s mutant plasmids were provided by P.-J. Chen (National Taiwan University College of Medicine, Taipei, Taiwan). Mouse CXCL9 or PD-L1 cDNA was inserted into the pLIVE vector (Mirus Bio) to force gene expression under the control of the mouse albumin promoter. To establish HBV-persistent mice, 6 µg HBV plasmid dissolved in 2.0 ml PBS was intravenously injected into mice within 5–6 s, as previously described (Xu et al., 2014).

Adoptive transfer, immune reconstitution, and vaccination. For the tolerance-transfer experiments, naive WT mice received an intravenous injection of 5×10^7 splenocytes followed by subcutaneous immunization with 2 µg HBsAg vaccine (adw subtype; BioKangtai Company) 1 d later. To reconstitute adaptive immunity, 2×10^7 splenocytes were adoptively transferred into naive Rag1$^{-/-}$ mice, and the recipients were then immunized 1 wk later with 2 µg HBsAg vaccine. To reconstitute CD4$^+$ T cell immunity, naive CD4$^{-/-}$ mice received adoptively transferred 5×10^7 splenocytes and were immunized with 2 µg HBsAg vaccine 1 d later.

Radioimmunoassay and [³H]thymidine incorporation. Serum HBsAg, HBeAg, and anti-HBs were measured using the corresponding radioimmunoassay kits (North Institute of Biological Technology) according to the manufacturer's instructions. [³H]thymidine ([³H]TdR) incorporation was performed to detect HBsAg-specific proliferation, as previously described (Zeng et al., 2013). Data were collected and expressed as the change in counts per minute (ΔCPM) of tritiated thymidine (ΔCPM = CPM of HBsAg-stimulated cells − CPM of unstimulated cells).

Cell isolation. Hepatic mononuclear cells, splenocytes, and lymph node cells were isolated as previously described (Zeng et al., 2013). Total CD4$^+$ T cell isolation was performed by magnetic activated cell sorting (MACS) using a mouse CD4$^+$ T cell isolation kit (Miltenyi Biotec). Hepatocyte and LNPC isolation was performed using a two-step in situ perfusion method followed by Percoll density gradient centrifugation, as previously described (Hou et al., 2009). Kupffer cells were isolated from LNPCs by MACS separation of F4/80$^+$ cells.

Cytometric bead array (CBA) assay. To detect IFN-γ, IL-2, IL-4, or IL-17A protein levels, 2×10^5 mononuclear cells or 10^5 CD4$^+$ T cells from the indicated organs of pAAV- or pAAV-HBV1.2–injected mice were separated and cultured in 96-well U-bottomed plates in the presence of 2 µg/ml anti-CD3 plus 1 µg/ml anti-CD28 for 96 h. In some indicated cases, CD4$^+$ T cells (10^5) were stimulated with 2 µg/ml HBcAg (ID LABS) or 5 µg/ml HBsAg (Hytest) in the presence of autologous irradiated splenocytes for 96 h. Supernatants were then collected, and cytokine levels were measured using their corresponding CBA kit (BD) according to the manufacturer's instructions. To detect CXCL9, a total of 10^5 hepatocytes, LNPCs, F4/80$^+$ Kupffer cells, or F4/80$^-$ LNPCs were cultured for 24 h; in some cases, the cells were cultured in the presence of 50 ng/ml recombinant mouse IFN-γ (PeproTech). Supernatants were also collected to measure CXCL9 protein levels using a CXCL9 CBA kit (BD). To measure the CXCL9 levels in liver, tissues were removed, weighed, and homogenized for CBA assay, as previously described (Hou et al., 2009).

Flow cytometry. This study used the following antibodies for flow cytometry (all from BD): FITC-conjugated anti–annexin V, anti-GL7, and anti-CD49d; PE-conjugated anti-CXCR3, anti-Fas, and anti-CD25; PerCP-Cy5.5–conjugated anti-B220 and anti-CD8; PE-Cy7–conjugated anti-NK1.1, anti-CD11a, and anti-CD45.1; allophycocyanin (APC)-conjugated anti-CD3; and APC-Cy7–conjugated anti-CD4 and anti-CD19. Alexa Fluor 647–conjugated anti-Foxp3 (BD) and PE-conjugated anti-Helios (BioLegend) antibodies were used for intracellular staining of T reg cells. Data were collected using a flow cytometer (LSR II; BD) and analyzed using FlowJo 7.6 software. To deplete NK1.1$^+$ cells, mice were intraperitoneally injected with 1 mg anti-NK1.1 (clone PK136; purified from HB-191 culture supernatants), and persistent NK1.1$^+$ cell depletion for at least 1 mo was confirmed by flow cytometry. For in vivo CXCR3, CTLA-4, or PD-L1 blockade, mice were injected intraperitoneally

with 200 µg of functional anti-CXCR3 (CXCR3-173; BioLegend), CTLA-4 (9H10; Bio X cell), or PD-L1 (10F.9G2; BioLegend) every other day.

Detection of HBsAg–specific CD4^{+} T cells. Customized I-A[b] tetramer loaded with HBsAg$_{126-138}$ peptide (RGLYFPAGG SSSG) was obtained from the National Institutes of Health tetramer core facility. I-A[b] tetramer loaded with human class II–associated invariant chain peptide (CLIP) was used as a negative control. For tetramer staining, hepatic mononuclear cells or splenocytes were incubated with 20 µg/ml tetramer at 37°C for 1 h in RPMI-1640 culture medium with 10% fetal bovine serum. The cells were then washed twice and stained for CD3, NK1.1, CD4, CD8, and 7-AAD. Tetramer^{+} cells were analyzed in the 7-AAD^{-}CD3^{+}NK1.1^{-}CD4^{+} population.

T reg cell suppression. Mouse T reg (CD4^{+}CD25^{+}) and effector T (CD4^{+}CD25^{-}) cells were isolated using a CD4^{+}CD25^{+} T reg cell isolation kit (Miltenyi Biotec) according to the manufacturer's instructions. For the [3H]TdR-based suppression assay, effector T cells were cocultured with an equal number of T reg cells in the presence of 2 µg/ml anti-CD3 plus 1 µg/ml anti-CD28 (10[5] cells + 10[5] cells/well in a 96-well U-bottomed plate) for 72 h, and [3H]TdR was added during the last 16 h, as previously described (Zeng et al., 2013).

Quantitative PCR and microarray assay. Total liver tissue RNA was isolated and reverse transcribed into cDNA, as previously described (Hou et al., 2009). Microarray analysis of gene expression in whole liver tissues was performed by eBioService using a Gene Chip (Affymetrix). Relative mRNA expression was measured using the SYBR Green (Takara Bio Inc.) staining method with a Rotor-Gene 6000 (Corbett Research) according to the manufacturer's instructions. The following PCR primer sequences were used in this study: *β-actin*, forward 5′-TGT GAT GGT GGG AAT GGG TCAG-3′ and reverse 5′-TTT GAT GTC ACG CAC GATTTCC-3′; *inos*, forward 5′-CAGCTGGGCTGTACA AACCTT-3′ and reverse 5′-CATTGGAAGTGAAGCGTT TCG-3′; *ido*, forward 5′-CCTTGA AGA CCA CCA CAT AG-3′ and reverse 5′-AGCACCTTTCGAACATCGTC-3′; *fasl*, forward 5′-CGGTGGTATTTTTCATGGTTCTGG-3′ and reverse 5′-CTT GTG GTT TAG GGG CTG GTT GTT-3′; *gal9*, forward 5′-GTT GTC CGA AAC ACT CAG AT-3′ and reverse 5′-ATATGATCCACACCGAGAAG-3′; *pdl1*, forward 5′-TGCTTCTCAATGTGACC-3′ and reverse 5′-GGAACAACAGGATGGAT-3′; *cxcl9*, forward 5′-GATAAGGAATGCACGATGCTC-3′ and reverse 5′-TCT CCGTTCAGTGTAGCAA-3′; *cxcl10*, forward 5′-CGA TGACGGGCCAGTGAGAATG-3′ and reverse 5′-TCA ACACGTGGGCAGGATAGGCT-3′; *cxcl11*, forward 5′-AATTTACCCGAGTAACGGCTG-3′ and reverse 5′-ATT ATGAGGCGAGCTTGCTTG-3′; *vcam1*, forward 5′-CTA CAAGTCTACATCTCTCCCAGGAA-3′ and reverse 5′-CCTCGCTGGAACAGGTCATT-3′; and *icam1*, forward

5′-TCGGAAGGGAGCCAAGTAACT-3′ and reverse 5′-GATCCTCCGAGCTGGCATT-3′.

REFERENCES

Berner, V., H. Liu, Q. Zhou, K.L. Alderson, K. Sun, J.M. Weiss, T.C. Back, D.L. Longo, B.R. Blazar, R.H. Wiltrout, et al. 2007. IFN-γ mediates CD4^{+} T-cell loss and impairs secondary antitumor responses after successful initial immunotherapy. *Nat. Med.* 13:354–360. http://dx.doi.org/10.1038/nm1554

Breous, E., S. Somanathan, L.H. Vandenberghe, and J.M. Wilson. 2009. Hepatic regulatory T cells and Kupffer cells are crucial mediators of systemic T cell tolerance to antigens targeting murine liver. *Hepatology.* 50:612–621. http://dx.doi.org/10.1002/hep.23043

Calne, R.Y., R.A. Sells, J.R. Pena, D.R. Davis, P.R. Millard, B.M. Herbertson, R.M. Binns, and D.A. Davies. 1969. Induction of immunological tolerance by porcine liver allografts. *Nature.* 223:472–476. http://dx.doi.org/10.1038/223472a0

Cao, O., E. Dobrzynski, L. Wang, S. Nayak, B. Mingle, C. Terhorst, and R.W. Herzog. 2007. Induction and role of regulatory CD4^{+}CD25^{+} T cells in tolerance to the transgene product following hepatic in vivo gene transfer. *Blood.* 110:1132–1140. http://dx.doi.org/10.1182/blood-2007-02-073304

Crispe, I.N. 2009. The liver as a lymphoid organ. *Annu. Rev. Immunol.* 27:147–163. http://dx.doi.org/10.1146/annurev.immunol.021908.132629

Crispe, I.N., T. Dao, K. Klugewitz, W.Z. Mehal, and D.P. Metz. 2000. The liver as a site of T-cell apoptosis: graveyard, or killing field? *Immunol. Rev.* 174:47–62. http://dx.doi.org/10.1034/j.1600-0528.2002.017412.x

Dikici, B., M. Bosnak, H. Ucmak, A. Dagli, A. Ece, and K. Haspolat. 2003. Failure of therapeutic vaccination using hepatitis B surface antigen vaccine in the immunotolerant phase of children with chronic hepatitis B infection. *J. Gastroenterol. Hepatol.* 18:218–222. http://dx.doi.org/10.1046/j.1440-1746.2003.02950.x

Dobrzynski, E., F. Mingozzi, Y.L. Liu, E. Bendo, O. Cao, L. Wang, and R.W. Herzog. 2004. Induction of antigen-specific CD4^{+} T-cell anergy and deletion by in vivo viral gene transfer. *Blood.* 104:969–977. http://dx.doi.org/10.1182/blood-2004-03-0847

Dong, H., G. Zhu, K. Tamada, D.B. Flies, J.M. van Deursen, and L. Chen. 2004. B7-H1 determines accumulation and deletion of intrahepatic CD8^{+} T lymphocytes. *Immunity.* 20:327–336. http://dx.doi.org/10.1016/S1074-7613(04)00050-0

Goubier, A., B. Dubois, H. Gheit, G. Joubert, F. Villard-Truc, C. Asselin-Paturel, G. Trinchieri, and D. Kaiserlian. 2008. Plasmacytoid dendritic cells mediate oral tolerance. *Immunity.* 29:464–475. http://dx.doi.org/10.1016/j.immuni.2008.06.017

1092

IFN-γ maintains liver-induced systemic tolerance | Zeng et al.

Hou, X., R. Zhou, H. Wei, R. Sun, and Z. Tian. 2009. NKG2D–retinoic acid early inducible-1 recognition between natural killer cells and Kupffer cells in a novel murine natural killer cell–dependent fulminant hepatitis. *Hepatology.* 49:940–949. http://dx.doi.org/10.1002/hep.22725

Huang, L.R., H.L. Wu, P.J. Chen, and D.S. Chen. 2006. An immunocompetent mouse model for the tolerance of human chronic hepatitis B virus infection. *Proc. Natl. Acad. Sci. USA.* 103:17862–17867. http://dx.doi.org/10.1073/pnas.0608578103

Jung, M.C., N. Grüner, R. Zachoval, W. Schraut, T. Gerlach, H. Diepolder, C.A. Schirren, M. Page, J. Bailey, E. Birtles, et al. 2002. Immunological monitoring during therapeutic vaccination as a prerequisite for the design of new effective therapies: induction of a vaccine-specific CD4+ T-cell proliferative response in chronic hepatitis B carriers. *Vaccine.* 20:3598–3612. http://dx.doi.org/10.1016/S0264-410X(02)00309-2

Kong, X., R. Sun, Y. Chen, H. Wei, and Z. Tian. 2014. γδT cells drive myeloid-derived suppressor cell–mediated CD8+ T cell exhaustion in hepatitis B virus–induced immunotolerance. *J. Immunol.* 193:1645–1653. http://dx.doi.org/10.4049/jimmunol.1303432

Lang, K.S., P. Georgiev, M. Recher, A.A. Navarini, A. Bergthaler, M. Heikenwalder, N.L. Harris, T. Junt, B. Odermatt, P.A. Clavien, et al. 2006. Immunoprivileged status of the liver is controlled by Toll-like receptor 3 signaling. *J. Clin. Invest.* 116:2456–2463. http://dx.doi.org/10.1172/JCI28349

Li, F., and Z. Tian. 2013. The liver works as a school to educate regulatory immune cells. *Cell. Mol. Immunol.* 10:292–302. http://dx.doi.org/10.1038/cmi.2013.7

Lin, Y.J., L.R. Huang, H.C. Yang, H.T. Tzeng, P.N. Hsu, H.L. Wu, P.J. Chen, and D.S. Chen. 2010. Hepatitis B virus core antigen determines viral persistence in a C57BL/6 mouse model. *Proc. Natl. Acad. Sci. USA.* 107:9340–9345. http://dx.doi.org/10.1073/pnas.1004762107

LoDuca, P.A., B.E. Hoffman, and R.W. Herzog. 2009. Hepatic gene transfer as a means of tolerance induction to transgene products. *Curr. Gene Ther.* 9:104–114. http://dx.doi.org/10.2174/156652309787909490

Lüth, S., S. Huber, C. Schramm, T. Buch, S. Zander, C. Stadelmann, W. Brück, D.C. Wraith, J. Herkel, and A.W. Lohse. 2008. Ectopic expression of neural autoantigen in mouse liver suppresses experimental autoimmune neuroinflammation by inducing antigen-specific Tregs. *J. Clin. Invest.* 118:3403–3410. http://dx.doi.org/10.1172/JCI32132

Maini, M.K., and A. Schurich. 2010. The molecular basis of the failed immune response in chronic HBV: therapeutic implications. *J. Hepatol.* 52:616–619. http://dx.doi.org/10.1016/j.jhep.2009.12.017

McDermott, D.S., and S.M. Varga. 2011. Quantifying antigen-specific CD4 T cells during a viral infection: CD4 T cell responses are larger than we think. *J. Immunol.* 187:5568–5576. http://dx.doi.org/10.4049/jimmunol.1102104

Mehal, W.Z., F. Azzaroli, and I.N. Crispe. 2001. Antigen presentation by liver cells controls intrahepatic T cell trapping, whereas bone marrow–derived cells preferentially promote intrahepatic T cell apoptosis. *J. Immunol.* 167:667–673. http://dx.doi.org/10.4049/jimmunol.167.2.667

Nebbia, G., D. Peppa, A. Schurich, P. Khanna, H.D. Singh, Y. Cheng, W. Rosenberg, G. Dusheiko, R. Gilson, J. ChinAleong, et al. 2012. Upregulation of the Tim-3/galectin-9 pathway of T cell exhaustion in chronic hepatitis B virus infection. *PLoS One.* 7:e47648. http://dx.doi.org/10.1371/journal.pone.0047648

Protzer, U., M.K. Maini, and P.A. Knolle. 2012. Living in the liver: hepatic infections. *Nat. Rev. Immunol.* 12:201–213. http://dx.doi.org/10.1038/nri3169

Refaeli, Y., L. Van Parijs, S.I. Alexander, and A.K. Abbas. 2002. Interferon γ is required for activation-induced death of T lymphocytes. *J. Exp. Med.* 196:999–1005. http://dx.doi.org/10.1084/jem.20020666

Rehermann, B., and M. Nascimbeni. 2005. Immunology of hepatitis B virus and hepatitis C virus infection. *Nat. Rev. Immunol.* 5:215–229. http://dx.doi.org/10.1038/nri1573

Schurich, A., P. Khanna, A.R. Lopes, K.J. Han, D. Peppa, L. Micco, G. Nebbia, P.T.F. Kennedy, A.-M. Geretti, G. Dusheiko, and M.K. Maini. 2011. Role of the coinhibitory receptor cytotoxic T lymphocyte antigen-4 on apoptosis-Prone CD8 T cells in persistent hepatitis B virus infection. *Hepatology.* 53:1494–1503. http://dx.doi.org/10.1002/hep.24249

Teijaro, J.R., C. Ng, A.M. Lee, B.M. Sullivan, K.C. Sheehan, M. Welch, R.D. Schreiber, J.C. de la Torre, and M.B. Oldstone. 2013. Persistent LCMV infection is controlled by blockade of type I interferon signaling. *Science.* 340:207–211. http://dx.doi.org/10.1126/science.1235214

Thomson, A.W., and P.A. Knolle. 2010. Antigen-presenting cell function in the tolerogenic liver environment. *Nat. Rev. Immunol.* 10:753–766. http://dx.doi.org/10.1038/nri2858

Tzeng, H.T., H.F. Tsai, H.J. Liao, Y.J. Lin, L. Chen, P.J. Chen, and P.N. Hsu. 2012. PD-1 blockage reverses immune dysfunction and hepatitis B viral persistence in a mouse animal model. *PLoS One.* 7:e39179. http://dx.doi.org/10.1371/journal.pone.0039179

von Oppen, N., A. Schurich, S. Hegenbarth, D. Stabenow, R. Tolba, R. Weiskirchen, A. Geerts, W. Kolanus, P. Knolle, and L. Diehl. 2009. Systemic antigen cross-presented by liver sinusoidal endothelial cells induces liver-specific CD8 T-cell retention and tolerization. *Hepatology.* 49:1664–1672. http://dx.doi.org/10.1002/hep.22795

Wang, Z., J. Hong, W. Sun, G. Xu, N. Li, X. Chen, A. Liu, L. Xu, B. Sun, and J.Z. Zhang. 2006. Role of IFN-γ in induction of Foxp3 and conversion of CD4+ CD25- T cells to CD4+ Tregs. *J. Clin. Invest.* 116:2434–2441. http://dx.doi.org/10.1172/JCI25826

Wilson, E.B., D.H. Yamada, H. Elsaesser, J. Herskovitz, J. Deng, G. Cheng, B.J. Aronow, C.L. Karp, and D.G. Brooks. 2013. Blockade of chronic type I interferon signaling to control persistent LCMV infection. *Science.* 340:202–207. http://dx.doi.org/10.1126/science.1235208

Wing, K., T. Yamaguchi, and S. Sakaguchi. 2011. Cell-autonomous and –non-autonomous roles of CTLA-4 in immune regulation. *Trends Immunol.* 32:428–433. http://dx.doi.org/10.1016/j.it.2011.06.002

Xu, L., W. Yin, R. Sun, H. Wei, and Z. Tian. 2013. Liver type I regulatory T cells suppress germinal center formation in HBV-tolerant mice. *Proc. Natl. Acad. Sci. USA.* 110:16993–16998. http://dx.doi.org/10.1073/pnas.1306437110

Xu, L., W. Yin, R. Sun, H. Wei, and Z. Tian. 2014. Kupffer cell–derived IL-10 plays a key role in maintaining humoral immune tolerance in hepatitis B virus–persistent mice. *Hepatology.* 59:443–452. http://dx.doi.org/10.1002/hep.26668

Zeng, Z., X. Kong, F. Li, H. Wei, R. Sun, and Z. Tian. 2013. IL-12–based vaccination therapy reverses liver-induced systemic tolerance in a mouse model of hepatitis B virus carrier. *J. Immunol.* 191:4184–4193. http://dx.doi.org/10.4049/jimmunol.1203449